IJE TRANSACTIONS A: Basics Vol. 25, No. 3, (July 2012) 231-238

International Journal of Engineering

Journal Homepage: www.ije.ir

Comparison of Lift and Drag Forces for Some Conical Bodies in Supersonic Flow Using Perturbation Techniques

A. B. Rahimi *

Professor, Faculty of Engineering, Ferdowsi University of Mashhad, P. O. Box No. 91775-1111, Mashhad, Iran

ARTICLE INFO

Article history:
Received 02 February 2010
Received in revised form 07 February 2012
Accepted 19 April 2012

Keywords:
Supersonic Flow
Conical Bodies
Lift to Drag Ratio
Squircle Cross-section
Euler Equations
Perturbation Techniques

ABSTRACT

Numerical methods are not always convergent especially in higher velocities when shock waves are involved. A comparison analysis is performed to study the supersonic flow over conical bodies of three different cross sections circular, elliptic and squircle (square with rounded corners) shaped using Perturbation techniques to find flow variables analytically. In order to find lift and drag forces the pressure force on the body is found, the component along x is drag and the component along z is lift. Three equations are obtained for lift to drag ratio of each cross section. The graphs for L/D show that for a particular cross section an increase in angle of attack, increases L/D. Comparing L/D in the three mentioned cross sections depicted that L/D is the greatest in squircle then in ellipse and the least in circle. The results are efficient in design of flying objects.
.

doi: *10.5829/idosi.ije.2012.25.03a.05*

NOMENCLATURE

a, b	semi-vertex of ellipse	s	entropy
c_p	pressure coefficient	u, v, w	velocity components
D	drag	x, y, z	Cartesian coordinate system
e	$=(a^2-b^2)/(a^2+b^2)$	Z	$=\theta/\delta$
F	function	**Greek letters**	
$\vec{F}$	pressure force	α	angle of attack
g_1	shock location coefficient	β	half shock angle
G_{11}, G_{12}, G_{13}	functions	γ	$=c_p/c_v$
H(0)	function	δ	half angle cone
J	constant	ρ	density
k_δ	$=M_\infty.\delta$	ε	perturbation parameter
L	lift	σ	$=\beta/\delta$
M	Mach number	ξ	constant
N	function	**Subscripts**	
n	coefficient	o	zero-order perturba tion
$\hat{n}$	unit normal vector	1	first-order perturbation
p	pressure	n	n -order perturbation
R	function	∞	free stream property
r, θ, ϕ	spherical coordinate system		

*Corresponding Author Email: *rahimiab@yahoo.com* (A. B. Rahimi)

1. INTRODUCTION

The flow past conical bodies has been studied for many different cases. A supersonic compressible three dimensional solution is useful in design of supersonic aircrafts, missiles, rockets and etc. Taylor-Maccoll [1] have investigated the steady supersonic flow past a right circular cone at zero angle of attack, they have reduced the governing equations to a single second-order nonlinear differential equation. Perturbation method is widely applied to studies of flow on conical bodies. Stone [2, 3] applied the power series expansion for a small angle of attack and obtained a solution via perturbation method. Sims [4] performed a numerical integration for Stone's solution.

Hypersonic flows over slender pointed nose elliptic cones at zero incidence is studied by Hemdan [5]. The flow is sought as a small perturbation from some basic circular cone flow. The geometry of the cone cross sections and surface velocities are expanded in Fourier series, using the supersonic linearized conical flow theory, the flow over slender pointed cones are calculated by Mascitti [6]. The analysis is similar to that of Doty and Rasmussen [7] and Rasmussen [8] for obtaining solutions for flow past circular cones at small angle of attack. The perturbation expansions which are used are not uniformly valid adjacent to body in the thin vortical layer, but it has been shown that pressure and azimuthal velocity components are valid across the vortical layer. First and second-order theory of supersonic flow past bodies of revolution have also been investigated by Van Dyke [9] and analytical solution for supersonic flow on a conical body of rounded triangle cross section via perturbation method has been done by Shekhi et al. [10].

The most recent studies in this subject are numerical investigation of supersonic flow for axisymmetric cones by Gross and Fasel [11] and also transient analysis of counterflowing jet over highly blunt cone in hypersonic flow by Barzegar et al. [12].

In this paper considering the Stone's perturbation expansions and applying them to three conical bodies with different cross sections as circle, ellipse and squircle at small angle of attack, the solution is obtained analytically. The purpose of the present work is to compare the lift to drag ratio for different cross sections, so calculating the flow variables for each case the pressure force is determined by integrating pressure around the body for an arbitrary length, then by calculating the dot product of the pressure force in x-direction and z-direction drag and lift forces are obtained respectively. The results will be useful in increasing the lift to drag ratio for aircrafts, satellites, missiles and space vehicles by changing the shape of the cross section or the angle of attack.

2. PROBLEM FORMULATION

Consider a supersonic flow over a conical body with arbitrary cross section. Spherical coordinate system is considered for this problem. Due to high Mach numbers, thin boundary layer and decrease of viscous effects, the governing equations become the Euler's equations.

It is assumed that the equation of the body is as follows:

$$\theta_c = \delta - \varepsilon \cos n\phi + o(\varepsilon^2) \tag{1}$$

$\theta_c = \delta$ is a cone with circular cross section in spherical coordinate system and semi-vertical angle of δ .The term $-\varepsilon \cos n\varphi$ is added to produce any arbitrary cross section by changing the values of ε and n, in which ε is a small parameter as a correction factor for cross section to achieve a convex cross section. This parameter is used as the perturbation factor in the expansions for flow variables and n determines the shape of cross section. Some of the most practical shapes are obtained by $n=1$, $n=2$ and $n=4$ which represent circle, ellipse and squircle cross sections respectively. Hence, hereafter these numbers 1, 2 and 4 indicate the shape of cross section. Writing the perturbation expansions the following relations are obtained for each flow variable, regarding previous studies in this field W0 is assumed to be negligible [13].

$$u(\theta,\varphi,\varepsilon) = u_0(\theta) + \varepsilon u_n(\theta)\cos n\varphi + o(\varepsilon^2) \tag{2}$$

$$v(\theta,\varphi,\varepsilon) = v_0(\theta) + \varepsilon v_n(\theta)\cos n\varphi + o(\varepsilon^2) \tag{3}$$

$$w(\theta,\varphi,\varepsilon) = \varepsilon w_n(\theta)\sin n\varphi + o(\varepsilon^2) \tag{4}$$

$$p(\theta,\varphi,\varepsilon) = p_0(\theta) + \varepsilon p_n(\theta)\cos n\varphi + o(\varepsilon^2) \tag{5}$$

$$\rho(\theta,\varphi,\varepsilon) = \rho_0(\theta) + \varepsilon \rho_n(\theta)\cos n\varphi + o(\varepsilon^2) \tag{6}$$

$$s(\theta,\varphi,\varepsilon) = s_0(\theta) + \varepsilon s_n(\theta)\cos n\varphi + o(\varepsilon^2) \tag{7}$$

Substituting the perturbation expansions in the Euler's equations and separating zero-order and first-order terms in ε, two systems of equations are obtained. Since there is no curvature along r, derivatives with respect to r are zero, so the systems of equations are simplified. To achieve a complete answer for flow over a conical body at small angle of incidence another perturbation expansion should be written for flow variables in which α (angle of incidence) is the perturbation factor,

$$u(\theta,\varphi,\alpha) = u_0(\theta) + \alpha u_2(\theta)\cos\varphi + o(\alpha^2) \tag{8}$$

$$v(\theta,\varphi,\alpha) = v_0(\theta) + \alpha v_2(\theta)\cos\varphi + o(\alpha^2) \tag{9}$$

$$w(\theta,\varphi,\alpha) = \alpha w_2(\theta)\sin\varphi + o(\alpha^2) \tag{10}$$

$$p(\theta,\varphi,\alpha) = p_0(\theta) + \alpha p_2(\theta)\cos\varphi + o(\alpha^2) \tag{11}$$

$$p(\theta,\phi,\alpha) = \rho_0(\theta) + \alpha\,\rho_2(\theta)\cos\phi + o(\alpha^2) \tag{12}$$

$$s(\theta,\varphi,\alpha) = s_0(\theta) + \alpha s_2(\theta)\cos\varphi + o(\alpha^2) \tag{13}$$

in this case the equation of the body is

$$\theta_c = \delta + \alpha\cos\varphi + o(\alpha^2) \tag{14}$$

Substituting the perturbation expansions with respect to α in the governing equations, separating zero-order and first-order terms in α, two systems of equations are obtained.

Superimposing the solutions for flow variables for each cross section with the solution of flow over a circular cone at small angle of incidence, a complete answer for arbitrary cross section at a small angle of incidence is obtained.

It is obvious that the systems of equations for zero-order in α and ε are similar to Equation (15).

$$\begin{cases} 2\rho_0 u_0 + (\rho_0 v_0)' + \rho_0 v_0\cot\theta = 0 \\ v_0 u_0' - v_0^2 = 0 \\ \rho_0 v_0 v_0' + \rho_0 u_0 v_0 + \dfrac{\partial p_0}{\partial\theta} = 0 \\ v_0 s_0' = 0 \\ s_0 = \ln\left(p_0 M_\infty^2\gamma\right) - \gamma\ln\rho_0 \\ \dfrac{1}{2}\left(u_0^2 + v_0^2\right) + \dfrac{\gamma}{\gamma-1}\dfrac{p_0}{\rho_0} - \dfrac{1}{2} - \dfrac{1}{(\gamma-1)M_\infty^2} = 0 \end{cases} \tag{15}$$

The following system accounts for the first-order terms in α (for $n=1$) and ε (for $n=2,4$). Where u, v, w are velocity components in r, θ, φ directions respectively, p the static pressure, ρ the density of the fluid, s is the entropy and M_∞ is the Mach number of the free stream.

Subscript (0) indicates solutions for the basic cone (circular cross section with no angle of attack), subscript $n=1$ denotes solutions for circular cone at none zero angle of incidence and for this case α is the perturbation factor. Subscripts $n=2,4$ respectively indicate solutions for ellipse and squircle cross sections and ε is the perturbation factor.

$$\begin{aligned} &2\left(\rho_0 u_n + u_0\rho_n\right) + \left(\rho_n v_0 + v_n\rho_0\right)' + \\ &+\cot\theta\left(\rho_0 v_n + v_0\rho_n\right) + \frac{n\rho_0 w_n}{\sin\theta} = 0 \\ &v_n u_0' + v_0 u_n' - 2v_0 v_n = 0 \\ &\rho_0\left(v_0 v_n\right)' + \rho_n v_0 v_0' + v_0\left(\rho_n u_0 + u_n\rho_0\right) + \\ &\rho_0 u_0 v_n + p_n' = 0 \\ &w_n' + \frac{u_0}{v_0} w_n + w_n\cot\theta - \frac{n}{\sin\theta}\frac{p_n}{\rho_0 v_0} = 0 \\ &v_0 s_n' + v_n s_0' = 0 \\ &s_n = \frac{p_n}{p_0} - \gamma\frac{\rho_n}{\rho_0} \\ &\frac{1}{2}\left(u_0^2 + v_0^2\right) + \left(u_n u_0 + v_n v_0\right)\frac{\rho_0}{\rho_n} + \frac{\gamma}{\gamma-1}\frac{p_n}{\rho_n} - \\ &-\frac{1}{2} - \frac{1}{(\gamma-1)M_\infty^2} = 0 \end{aligned} \tag{16}$$

From the first system the following differential equation with respect to u_0 is achieved,

$$u_0'' + u_0'\cot\theta + 2u_0 = 0 \tag{17}$$

The second system of equations leads to the following differential equation with respect to un

$$u_n'' + u_n'\cot\theta + u_n\left(2 - \frac{n^2}{\sin^2\theta}\right) = -\frac{n^2 F_n}{\gamma}\frac{H_0(\theta)}{\sin^2\theta} \tag{18}$$

The boundary conditions at the body surface are described by the tangency condition.

$$v_0(\delta) = v_1(\delta) = 0 \tag{19}$$

To solve the above differential equations two boundary conditions are required for each equation, from mass conservation across the shock and normal to the shock, the velocity components at the shock are achieved as the following, Equations (20) and (21) are the boundary conditions at the shock for Equation (17) according to the system of Equations (15),

$$u_0(\beta) = \cos\beta \tag{20}$$

$$v'_0(\beta) = -\left(1 + \frac{1}{\sigma^2}\right) \tag{21}$$

$$u_1(\beta) = \delta\sin\beta\left(1 - g_1(1-\xi_0)\right) \tag{22}$$

$$u_1'(\beta) = -\delta g_1 v'_0(\beta) + \delta\xi_0\cos\beta\left(1 - g_1\right) - \xi_1\sin\beta \tag{23}$$

$$\xi_0 = 1 - \frac{1}{\sigma^2} \tag{24}$$

For small angles Equation (17) is solved as follows,

$$\frac{u_0(\theta)}{u_\infty} = 1 - \frac{\theta^2}{2} + (1-\xi_0)(\beta^2)\ln\left(\frac{\theta}{\beta}\right) \tag{25}$$

$$\frac{v_0(\theta)}{u_\infty} = -\theta\left[1 - (1-\xi_0)\frac{\beta^2}{\theta^2}\right] \tag{26}$$

$$P_0(\theta) = \frac{1}{\gamma}\left(\frac{M_\infty^2}{\exp(s_0)}\right)^{\frac{1}{\gamma-1}}\left[\frac{1}{2}(\gamma-1)\left(1 - u_0^2 - v_0^2\right) + \frac{1}{M_\infty^2}\right]^{\frac{\gamma}{\gamma-1}} \tag{27}$$

$$\rho_0(\theta)=\left[\frac{M_\infty^2}{\exp(s_0)}.\left\{\frac{1}{2}(\gamma-1)\left(1-u_0^2-v_0^2\right)+\frac{1}{M_\infty^2}\right\}\right]^{\frac{1}{\gamma-1}} \quad (28)$$

For small angles Equation (18) is also solved as follows,

$$\overline{u_1}(Z)=\frac{u_1(z)}{\delta^2}=G_{11}Z-G_{12}\frac{1}{Z}+G_{13}R \quad (29)$$

$$\overline{v_1}(Z)=\frac{v_1(Z)}{\delta}=G_{11}+G_{12}\frac{1}{Z^2}+G_{13}\frac{dR}{dZ} \quad (30)$$

Where

$$G_{11}=\frac{1}{2\sigma^2}+\frac{\gamma-1}{\gamma+1}+g_1\left(\frac{2}{\gamma+1}-\frac{1}{2\sigma^2}\right) \quad (31)$$

$$G_{12}=\left(\frac{1}{2}-\frac{2\sigma^2}{\gamma+1}\right)+g_1\left(\frac{1}{2}+\frac{2\sigma^2}{\gamma+1}\right)+\frac{(1-g_1)}{4\sigma^2}J \quad (32)$$

$$G_{13}=\frac{(1-g_1)J}{\sigma^3}=\frac{F_1J}{N\gamma} \quad (33)$$

$$R=1-\frac{3}{4}\left(\frac{\sqrt{z^2-1}}{\sqrt{\sigma^2-1}}\right)+\frac{2Z^2+1}{4Z}\frac{\ln\left(\overline{Z}/\overline{\sigma}\right)}{\sqrt{\sigma^2-1}} \quad (34)$$

In which $\overline{\sigma}=\sigma+\sqrt{\sigma^2-1}$, $\overline{Z}=Z+\sqrt{z^2-1}$.

$$N=\frac{2\sigma^2}{(\sigma^2-1)(2\sigma^2+\gamma-1)} \quad (35)$$

$$J=\frac{2\sigma^2\left[\sigma^2-1+(\gamma-1)\ln\sigma\right]}{(\sigma^2-1)(2\sigma^2+\gamma-1)} \quad (36)$$

$$F_1=\frac{\gamma(1-g_1)N}{\sigma^3} \quad (37)$$

$$z=\frac{\theta}{\delta}\qquad \sigma=\frac{\beta}{\delta} \quad (38)$$

By use of the boundary condition:

$$\overline{v_1}(1)=0 \quad (39)$$

Shock eccentricity caused by the angle of attack is obtained as the following,

$$g_1=\{2+J+2\sigma^2[3-\frac{4(\sigma^2+1)}{\gamma+1}]- (\frac{J}{\sigma\sqrt{\sigma^2-1}})\ln(\bar{\sigma})\}/\{4+J-2(\sigma^2+1)[1+\frac{4\sigma^2}{\gamma+1}]-(\frac{J}{\sigma\sqrt{\sigma^2-1}})\ln(\bar{\sigma})\} \quad (40)$$

$$p_1(\theta)=F_1p_0(\theta)-\rho_0(\theta).\left[u_0(\theta)u_1(\theta)+v_0(\theta)v_1(\theta)\right] \quad (41)$$

To find lift to drag ratio calculations show that

$$p_0(\delta)=p_\infty\left(1+\frac{\gamma}{2}k_\delta^2\left(1+\frac{\sigma^2\ln\sigma^2}{\sigma^2-1}\right)\right) \quad (42)$$

$$\frac{c_{p_0}}{\delta^2}=1+\frac{\sigma^2\ln\sigma^2}{\sigma^2-1} \quad (43)$$

$$\frac{c_{p_1}}{\delta}=\frac{2N}{k_\delta^2}\left(1+\frac{\gamma}{2}k_\delta^2\left(1+\frac{\sigma^2\ln\sigma^2}{\sigma^2-1}\right)\right).\left(\frac{1-g_1}{\sigma^3}-\frac{a_0^2(\beta)}{a_0^2(\delta)}\frac{u_1(\delta)}{V_\infty\delta}\right) \quad (44)$$

$$\frac{u_1(\delta)}{V_\infty\delta}=-2+\frac{(1-g_1)}{\sigma^3}.\left[\frac{4\sigma^2}{\gamma+1}+\sigma^3-\frac{\sigma^2}{2}+1-\frac{\ln\left(\sigma+\sqrt{\sigma^2-1}\right)}{2\sqrt{\sigma^2-1}}\right] \quad (45)$$

$$\frac{a_0^2(\beta)}{a_0^2(\delta)}=1+\frac{(\gamma-1)\sigma^2\left[\ln\sigma^2+\frac{1}{\sigma^2}-1\right]}{(\sigma^2-1)(2\sigma^2+\gamma-1)} \quad (46)$$

$\frac{c_{p_0}}{\delta^2}$ and $\frac{c_{p_1}}{\delta}$ fare shown in Figures (1) and (2) as the following.

Comparisons of the pressure coefficient from our study with the existing studies are depicted in the two following Figures (3) and (4), which proves well. The numerical results are Sim's results [4] and also a Fluent CFD software has been used by present author to model the three Dimensional cone.

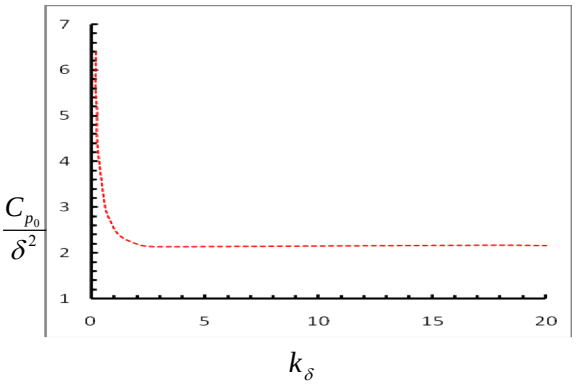

Figure 1. cp_0/δ^2 versus k_δ

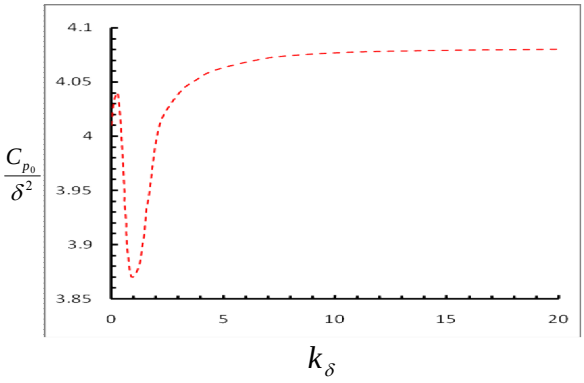

Figure 2: cp_1/δ versus k_δ

A grid dependence study was conducted to arrive at tetrahedral grid size for optimal accuracy and efficiency for laminar and turbulent cases. For modeling of Reynolds stress in momentum equation, RNG k-ε turbulence model has been used.

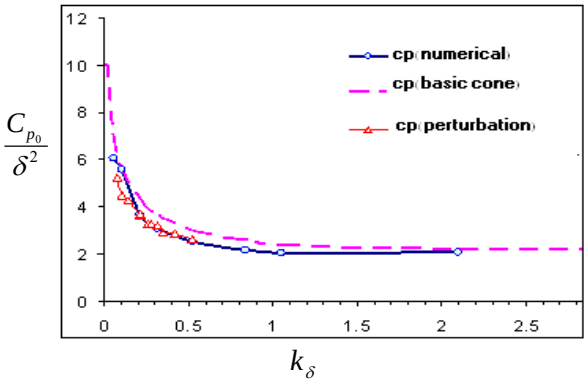

Figure 3. C_p/δ^2 vs. k_δ in numerical and analytic solution

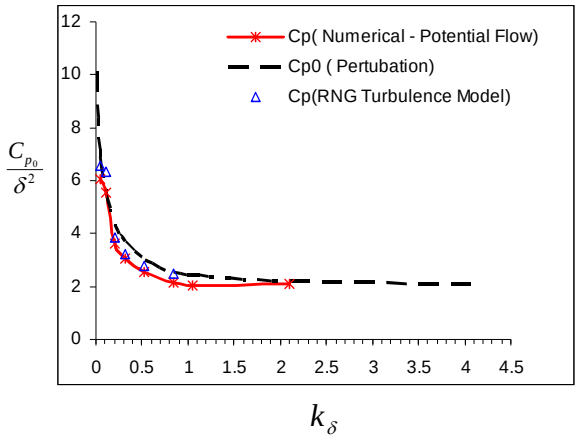

Figure 4. Analytic solution and numerical solution (basic cone)

3. CALCULATING LIFT AND DRAG FORCES

The pressure force on a finite-length cone is given by

$$\vec{F} = -\iint_s p(\theta_c)\hat{n}dS \tag{47}$$

$$\hat{n} = \hat{e}_\theta - \frac{n\varepsilon \sin n\varphi}{\sin\delta}\hat{e}_\varphi + o(\varepsilon^2) \tag{48}$$

$$dS = r\sin\theta_c dr d\varphi + o(\varepsilon^2) \tag{49}$$

The equations for *Lift* and *drag* forces are as follow:

$$D = \vec{F}\cdot\hat{e}_z = p_0(\delta)\pi H^2\tan^2\delta + o(\varepsilon^2) \tag{50}$$

$$L = \vec{F}\cdot\hat{e}_x = -\frac{1}{4}\frac{c_{p_1}}{\delta}\alpha\gamma M_\infty{}^2 p_\infty \pi H^2\tan^2\delta + o(\alpha^2,\varepsilon^2,\alpha\varepsilon) \tag{51}$$

$$\frac{L}{D} = -\frac{1}{4\delta}\frac{c_{p_1}\alpha\gamma M_\infty{}^2 p_\infty}{p_0(\delta)} \tag{52}$$

4. RESULTS AND DISCUSSION

For comparing the lift to drag ratio in different cross sections, first the relation between δ and the shape of cross section should be found.

In rectangle Cartesian coordinates, an elliptic cone is represented by:

$$\frac{x^2}{a^2z^2} + \frac{y^2}{b^2z^2} = 1 \tag{53}$$

where,

Cartesian to spherical transformers are

$$x = r\sin\theta\cos\varphi \tag{54}$$

$$y = r\sin\theta\sin\varphi \tag{55}$$

$$z = r\cos\theta \tag{56}$$

Substituting Equations (54-56) in Equation (53) the following relations are obtained.

$$\tan\theta = \frac{\tan\theta_m}{\sqrt{1+e\cos 2\varphi}} \tag{57}$$

In which

$$\tan\theta_m = \frac{\sqrt{2}ab}{\sqrt{a^2+b^2}} = b\sqrt{1-e} \tag{58}$$

$$e = \frac{b^2-a^2}{b^2+a^2} \tag{59}$$

In the left hand side of Equation (58), the Taylor expansion about ε=0 is written and in right hand side the Fourier series are substituted. For different values of e calculations shows that Fourier series coefficients except for a_0 and a_2 are negligible, so the following equation is achieved.

$$\tan\delta - \varepsilon(1+\tan^2\delta)\cos 2\phi = \tan\theta_m\left(\frac{a_0}{2} + a_2\cos 2\phi\right) \tag{60}$$

where,

$$a_0 = \frac{1}{\pi}\int_{-\pi}^{\pi}\frac{1}{\sqrt{1+e\cos 2\varphi}}d\varphi \tag{61}$$

$$a_2 = \frac{1}{\pi}\int_{-\pi}^{\pi}\frac{\cos 2\varphi}{\sqrt{1+e\cos 2\varphi}}d\varphi \tag{62}$$

On the other hand $a_0 \approx 1$ then for small angles and comparing the two sides of Equation (60) the two following relations are obtained.

$$\delta = b\sqrt{1-e} \tag{63}$$

$$\varepsilon = -\frac{a_2\tan\theta_m}{1+b^2(1-e)} \tag{64}$$

It is obvious that for a circular cone, $e=0$.

$$\delta = b \tag{65}$$

$$\varepsilon = 0 \tag{66}$$

In rectangle Cartesian coordinates, a cone with squircle cross section is represented by

$$\frac{x^4}{z^4}+\frac{y^4}{z^4}=R^4 \tag{67}$$

The Cartesian to Spherical Transformers are substituted in the Cartesian equation of squircle,

$$\tan\theta_c=\frac{\sqrt{2}R}{(3+\cos 4\varphi)^{1/4}} \tag{68}$$

Using Equation (1) and Taylor Expansion about $\varepsilon=0$ for the left hand side of Equation (68) and writing Fourier series for the right hand side, the following relation is obtained.

$$\tan\delta-\varepsilon(1+\tan^2\delta)\cos 4\phi=\frac{a_0}{2}+a_4\cos 4\phi \tag{69}$$

In comparison with a_0 , a_4 the other coefficients of the Fourier series are much smaller and hence negligible.

Comparing the two sides of Equation (69) the following relations are achieved.

$$\tan\delta=\frac{a_0}{2} \tag{70}$$

$$\varepsilon=-\frac{a_4}{1+(\frac{a_0}{2})^2} \tag{71}$$

In which

$$a_0=\frac{1}{\pi}\int_{-\pi}^{\pi}\frac{\sqrt{2}R}{(3+\cos 4\varphi)^{1/4}}d\varphi \tag{72}$$

$$a_4=\frac{1}{\pi}\int_{-\pi}^{\pi}\cos 4\varphi\frac{\sqrt{2}R}{(3+\cos 4\varphi)^{1/4}}d\varphi \tag{73}$$

R is a constant and equals to the radius of a circle tangent to the inner side of the squircle. The *lift to drag ratio* versus k_δ is shown the following figures, where for small angle of attack.

$$k_\delta=M_\infty\delta \tag{74}$$

As the angle of attack increases, the *lift to drag ratio* trends to a constant value for a greater value of k_δ and the value of this constant increases with the increase in angle of attack.

In Figures (5-7) comparing the lift to drag ratio it is seen that increasing n from 1 to 4 causes an increase in L/D, for an ellipse and a squircle which are tangent to the inner side of a circle the lift to drag ratio respectively increases and trends to a constant value which is the greatest for a squircle. Also as it can be seen from the figures and also in Equation (74) which known as the hypersonic small disturbance parameter, since semi vertical angle of cone is small, the values of k_δ more than 5 is considered infinity.

As expected by decreasing the semi-vertical angle of the cones as shown in Figure (7), the lift to drag ratio has increases for all of the cross sections because the flow encounters a more slender body.

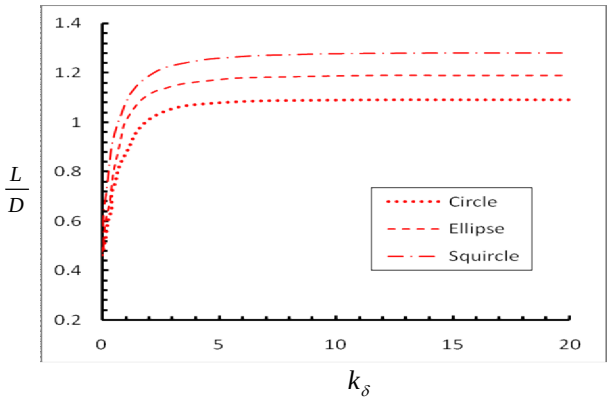

Figure 5. lift to drag ratio versus k_δ, α=4°, semi vertical angle of tangent circular cone is 14.3°

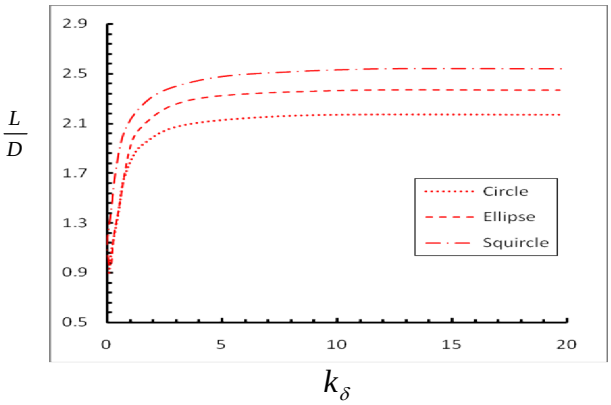

Figure 6. lift to drag ratio versus k_δ, α=8°, semi vertical angle of tangent circular cone is 14.3°

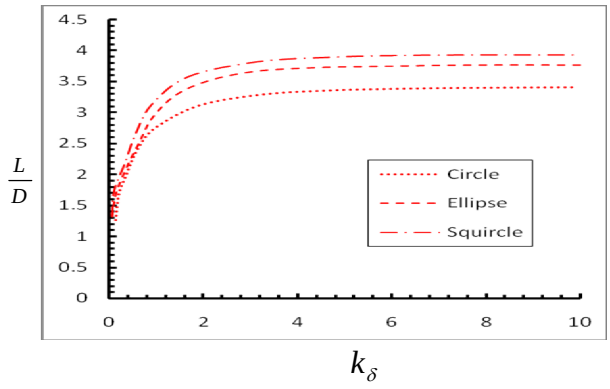

Figure 7. lift to drag ration versus k_δ, α=8°, semi vertical angle of tangent circular cone is 11.5°

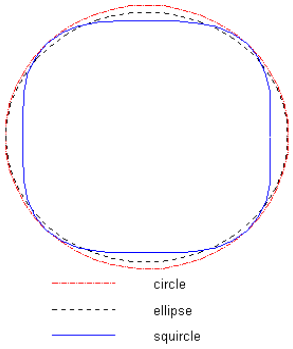

Figure 8. Positioning of cross sections for comparing lift to drag ratio.

5. CONCLUSIONS

The perturbation method was applied to analytically obtain flow variables over conical bodies of three different cross sections, circle, ellipse and squircle. The aim of the present work is to improve lift to drag ratio by changing the cross section of the conical body. Using Fourier series a relation between δ and the shape of the cross section of the body is obtained for each case. These relations show that by changing the cross section from a circle to an ellipse then to a squircle in a manner that the ellipse and squircle is tangent to the inner side of the circle and the ellipse lies between the other two shapes, Figure (8), the lift to drag ratio increases. L/D will also increment if the angle of attack increases. Also as it can be seen from the figures and Equation (74) known as the hypersonic small disturbance parameter, since semi vertical angle of cone is small, the values of k_δ more than 5 is considered infinity.

6. REFERENCES

1. Taylor, G. I. and Maccoll, J. N., "The air pressure on cones moving at high speeds", ***Proceeding of the Royal Society of London Series A,*** Vol. 139, (1933), 278-311.
2. Stone, A. H., "on supersonic flow past a slightly yawing cone", ***Journal of Mathematics and Physics (I)***, Vol. 27, (1948), 67-81.
3. Stone, A. H., "on supersonic flow past a slightly yawing cone", ***Journal of Mathematics and Physics (II)***, Vol. 30, (1952), 220-233.
4. Sims, J. L., "Tables for supersonic flow around right circular cones at small angle of attack", NASA, SP-3007, 1964.
5. Hemdan, H. T., "Hypersonic flows over slender pointed-nose elliptic cones at zero incidence", ***Journal of Acta Astronautica,*** Vol. 45, No. 1, (1999), 1-10.
6. Mascitti, R., "Calculation of linearized supersonic flow over slender cones of arbitrary cross section", NASA, TN D-6818, 1972.
7. Doty, R. T. and Rasmussen, M. L., "approximation for hypersonic flow past an inclined cone", ***Journal of the American Institute of Aeronautics and Astronautics (AIAA),*** Vol. 11, No. 9, (1973).
8. Rasmussen, M. L., "Hypersonic Flow", John Wiley & Sons, Inc., New York, 1994.
9. Van Dyke, M. D., "First and second-order theory of supersonic flow past bodies of revolution", ***Journal of Spacecraft and Rockets,*** Vol. 40, No. 6, (2003), 1029-1047,
10. Shekhi, N. and Rahimi, A. B., "Analytical solution for supersonic flow on a conical body of rounded triangle cross-section via the perturbation method", The 7th ISME/WSEAS International Conference, Moscow, Russia, 2009.
11. Gross A. and Fasel, H. F., "Numerical investigation of supersonic flow over axisymmetric cones", ***Mathematics and Computers in Simulation***, Vol. 81, Issue 1, (2010), 133-142.
12. Barzegar, M., Bishehsani, S., Hossienalipour, S. M. and Sedighi, K., "Transient analysis of counterflowing jet over highly blunt cone in hypersonic flow", ***Acta Astronautica***, (2011).
13. Tsai, B. J. and Chou,Y. T., "Analyzing the longitudinal effect of hypersonic flow past a conical cone via the perturbation method", ***Journal of Applied Mathematical Modeling***, Vol. 32, No. 12, (2008), 2596-2620.

Comparison of Lift and Drag Forces for Some Conical Bodies in Supersonic Flow Using Perturbation Techniques

A. B. Rahimi

Professor, Faculty of Engineering, Ferdowsi University of Mashhad, P. O. Box No. 91775-1111, Mashhad, Iran

A R T I C L E I N F O

Article history:
Received 02 February 2010
Received in revised form 07 February 2012
Accepted 19 April 2012

Keywords:
Supersonic Flow
Conical Bodies
Lift to Drag Ratio
Squircle Cross-section
Euler Equations
Perturbation Techniques

چکیده

روش‌های محاسبات عددی و به‌خصوص در سرعت‌های بالاتر که در آن جریان همراه با موج‌های ضربه‌ای همراه می‌باشند قابلیت همگرائی را ندارند. در این تجزیه و تحلیل جریان مافوق صوت بر روی اجسام مخروطی شکل با سه سطح مقطع متفاوت دایروی، بیضوی، و مربعی با گوشه‌های گرد مورد مطالعه قرار گرفته است. روش پرتوربیشن برای به‌دست آوردن کمیات جریان به صورت تحلیلی مورد استفاده قرار می‌گیرد. جهت به‌دست آوردن نیروهای برا و پسا باید نیروی فشار بر روی جسم را به‌دست آورد. مولفه این نیرو در جهت X نیروی پسا و در جهت Z نیروی برا می‌باشد. سه رابطه برای نسبت نیروی برا به پسا برای سه سطح مقطع یاد شده به‌دست می‌آید. از رسم این نسبت‌ها برای سطوح مقطع متفاوت، همان‌طور که انتظار می‌رود، مشاهده می‌شود که این نسبت با افزایش زاویه حمله افزایش می‌یابد. از مقایسه این نسبت برای سه سطح مقطع مذکور مشاهده می‌شود که بزرگترین آن برای سطح مقطع مربعی با گوشه‌های گرد و سپس سطح مقطع بیضوی و کمترین آن مربوط به سطح مقطع دایروی می‌باشد. این نتایج جهت بهینه سازی طراحی اجسام پرنده مورد استفاده قرار می‌گیرند

doi: *10.5829/idosi.ije.2012.25.03a.05*